AUT Journal of Electrical Engineering

AUT J. Elec. Eng., 49(1)(2017)85-94
DOI: 10.22060/eej.2016.12054.5030

Evaluation of Geometric and Atmospheric Doppler for GNSS-RO Payloads

L. Mohammadi, S. Amiri*, G.R. MohammadKhani

Iranian Research Organization for Science & Technology, Tehran, Iran

ABSTRACT: To reduce the sampling rate in global navigation satellite system (GNSS)-radio occultation receivers, it is essential to establish a suitable estimation of Doppler frequency from the received signal in the satellite onboard receiver. This receiver is usually located on low earth orbit satellite and receives GNSS satellites signal in the occultation situation. The occurred Doppler on the signal contains the Geometric and Atmospheric segments. The Geometric Doppler's value depends on the orbital situation of transmitter and receiver. However, Atmospheric Doppler depends on the signal propagation environment conditions. To investigate the nature of these two types of doppler, we establish different missions on STK software environment for receivers located on different orbits from 450km altitude to 800km and 1500km with different orbital parameters and by considering the Global Positioning System satellites as the transmitters. We also study the value and nature of the atmospheric doppler by utilizing and analyzing the data produced by the COSMIC Data Analysis and Archive Databases Center. In signal tracking part of the receiver, the variation of Doppler is also important, in addition to the Doppler that is called phase acceleration. Therefore, the derivatives of Geometric Doppler related to the LEO satellites in different altitudes need to be considered.

Review History:

Received: 18 October 2016
Revised: 15 November 2016
Accepted: 27 February 2017
Available Online: 2 March 2017

Keywords:
Atmospheric and Geometric Doppler
Open-loop tracking
radio occultation
Phase acceleration

1- Introduction

A. State of the Art

Retrieving Atmospheric parameters from radio wave signal variations traversing planetary atmospheres was demonstrated with the Mariner mission in 1960. The occultation occur when the emitted signal from the transmitter, received in the receiver after crossing the atmosphere whereas they aren't in line of sight, is called radio occultation (RO).

The availability of the Global Navigation Satellite System (GNSS) constellations, such as, the Global Positioning System (GPS), GALILEO, BeiDou and others, offers an affordable way to operate radio occultation method for sounding the earth's atmosphere. A radio occultation receiver is usually located on a Low Earth Orbiting (LEO) satellite to track GNSS signals. There are some experiments of occultation by Airplane and on top of mountain. Fig.1 shows the signal trajectory in an occultation event and demonstration of related parameters. As it can clearly be seen, the signal is bent and therefore travels a longer distance than a straight line and causes more delay in signal phase.

Due to the knowledge of the transmitted signal features and also through calculating the features of the received signal, we can determine the propagation environment (atmosphere) parameters. Atmosphere sounding by means of GNSS-RO improves numerical weather prediction and climate change studies. So the recorded phase and amplitude of the radio waves during the occultation can be analyzed to determine neutral Atmospheric parameters, including refractivity, water vapor pressure, temperature, and humidity, as well as ionospheric total electron content [1].

Propagation of RO signals through the moist troposphere results in multipath and strong fluctuation of the phase and amplitude. Therefore, tracking such signals by PLL may result in large deviation of the signal phase from the phase model, updated with the use of feedback from the received signal [2]. This, in turn, results in random and systematic error (bias) in the extracted phase and in the retrieved refractivity profile. Moreover, the PLL tracking of the multi tone RO signals is unstable. Instability of the PLL tracking in the moist troposphere motivated to consider the OL tracking [3], [4] and [5] so in the conditions that the variations of the signal are intensive, the Open-Loop (OL) technique is applied to acquire the signal. This method relies on a priori models of Doppler and needs the position of the transmitter and receiver and also estimation of atmospheric conditions that are used in Doppler model section in receiver.

B. Related Works

At the first, the open-loop tracking implemented on Scientific Application Satellite-C (SAC-C) and later adapted on constellation observing system for meteorology, ionosphere, and climate (COSMIC) launched in April 2006[6].

In a recent study [7] of occultation events from the six-spacecraft COSMIC constellation (also known as FORMOSAT-3) [8] show valuable information especially for climate trend detection. In addition, assimilation of GPS-RO measurements in numerical weather prediction models have been demonstrated to yield positive impacts on the forecasts and leading to the operational use of COSMIC data at European Center for Medium-range Weather Forecasts (ECMWF), national center for environmental prediction (NCEP), and other weather centers around the world since 2006 [9], [10].

Analysis of doppler frequency results in ± 50 kHz and ± 2kHz geometric and atmosphere Doppler, respectively [3] and [2]. Authors estimate Atmospheric Doppler based on the

Corresponding author; Email: amiri@irost.org

variations of amplitude and phase of the received signal. In terms of reproducing the temperature and moisture profile in the lowest 2.5 km, statistical analysis is performed on a large number of COSMIC profiles in a region surrounding Macquarie Island [11].

The estimations of the quantity of filter bandwidth and sampling rate are principles of the RO receiver, it is more important in OL mode receiver. In real time, a RO signal must be subject to down-conversion in receiver, by use of the pre-calculated phase model, without a feedback from the received signal. The down-converted RO signal is low-pass filtered, sampled and transmitted to the ground for post processing. In previous related works, the sliding window method is used for estimation of doppler frequency, which is one of Radio Holographic (RH) methods.

To improve retrieval accuracy in the moist lower troposphere, RH methods are suggested to process RO data in atmospheric multipath zones: back propagation (BP) [12,13], sliding spectral (SS) [3], canonical transform (CT) [14,15] , full spectrum inversion (FSI) [16], CT2 [17] and phase matching (PM) [18]. These techniques, presume that the occulted signal phase and amplitude are accurately recorded by the GPS receiver, a condition which has proven to be very difficult to satisfy. Various issues associated with tracking the GPS signal in the lower troposphere have been addressed in the literature [3, 19, 20].

SS method takes into account the whole spectral content of the signals in the small aperture. Different frequency estimation methods such as multiple signal classification (MUSIC) technique were used to test SS method by processing 4 GPS/Meteorology (MET) occultation [21]. By spectral analysis, the contributions from components of surface reflections were detected in 20% to 30% of CHAMP (Challenging Minisatellite Payload) occultations. Sokolovskiy et al. in [22] thoroughly investigated the bias induced by the noise in RH methods, and gave a physical explanation. However, false spectral maxima induced by the noise can often result in retrieval errors in SS method. Therefore, accuracy of frequency estimation is very important in SS and other methods.

In occulted GPS signal tracking, the most challenging problem has been the accurate detection of the occulted GPS signal in the lower troposphere. The data from this region are either missing or containing errors that, if unaccounted for, could cause large errors and biases in the retrieved refractivity profiles in the lower troposphere. It is believed that tracking errors were the dominant source of the refractivity bias observed with GPS/MET data [23], and later in the CHAMP and SAC-C data [24,19, 25]. Another source of the negative refractivity bias is thought to be arising from non-uniqueness problem affecting Abel inversion in the presence of elevated ducts or so-called super refraction layers [26,19,27,28].

In [6], the authors investigate how well they can predict the Doppler shift and the delay induced by the atmosphere on the occulted signal and describe the specific implementation of OL tracking on SAC-C for both setting and rising occultations. In [29], the author focused on the free troposphere. At altitudes above 3 km biases are caused by deviations of the refractivity field from spherical symmetry and receiver induced tracking errors. The results of simulations studies' results indicate that within regions of low signal-to-noise ratios, a promising signal detection technique is bandwidth reduction of the receiver's carrier tracking loop.

Considering typical spectral bandwidth from tropical tropospheric RO signals, analysis from [3], shows that Atmospheric Doppler is 1 kHz. In this paper, we will investigate the Atmospheric Doppler by utilizing the data produced by the COSMIC Data Analysis and Archive Center (CDAAC) databases for different atmospheric conditions. Studying of range and nature of atmospheric and geometric doppler is very important in the prediction of doppler models in OL tracking .and receiver bandwidth calculations affected by doppler.

C. The new proposed method

In this paper, we investigate the nature of geometric and Atmospheric Doppler. In this regard, we establish different missions on STK software environment for receivers located on different orbits. The main results and original contributions of this paper are the following:

- We establish different missions on STK software environment for receivers located on different orbits from 450 km altitude to 800 km and 1500 km with different orbital parameters.
- We study the value and nature of the Atmospheric Doppler and provide the analytical results by utilizing the data produced by the CDAAC databases.
- Despite the number listed in [3], by examining the value of Atmospheric and Geometric Doppler by data produced by the CDAAC databases, we will show that Atmospheric Doppler is higher in the lower moist troposphere. This issue can be used in modelling Atmospheric Doppler on OL tracking.

This paper is organized as follows. In Section 2, we investigate RO signal processing by using OL tracking. Then, we investigate the Atmospheric and Geometric Doppler model in Sections 3 and 5, respectively. Conclusions are presented in Section 7.

2- Open-loop tracking in RO

Atmospheric parameters like vapor, pressure and temperature cause variation in the amount of bending angle. Excess Doppler (Refractivity) is extracted from the bending angle. Open-loop tracking is based on the raw sampling of the received signal. This method relies on the Doppler estimation model and as the precision of Doppler estimation Model. While the precision increases, the sampling rate is reduced. Thus, the bandwidth required to send the information to Earth for post-processing decreases.

In fact, the high sampling rate of the raw measurement enables a monitoring of the high frequency fluctuations and improves the spatial resolution of the refractivity profile. However, high sampling rate would demand huge amounts of data and require intensive ground-based processing and additional cost. Therefore, due to the cost and bandwidth constraints and limitation on the amount of information sent to the post-processing, reducing the sampling rate is considered. In this paper, in section III we suggest a fast and convenient way to obtain the Atmospheric Doppler by the archived data of databases for using in Atmospheric Doppler model and decreasing the sampling rate. Table 1 shows the sampling rate with respect to the model and the transmitted information size[6]. Note that these sampling rates and their comments are obtained by simulations and the maximum sampling rate that has been achieved to date is 100 Hz

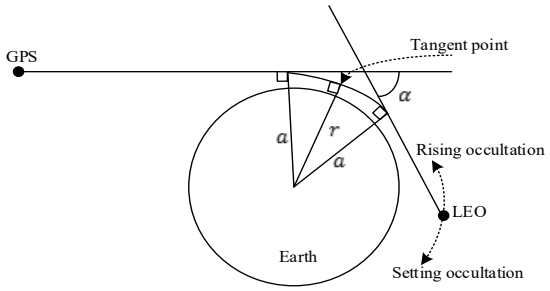

Fig. 1. A radio occultation event (α: Bending Angle a: Impact Parameter)

with the CASSIOPE RO mission.

Due to the fast phase/frequency variations, low signal to noise ratio, and multipath event in lower troposphere altitudes, signal tracking is not possible by the closed-loop method. This issue is worse in the event of rising occultation, because acquisition and tracking of signal starts with very weak signals.

Another important issue is the sufficiency of only using L1 coarse acquisition (C/A) frequency, for determining low atmosphere layer parameters, because there is the weaker strength of the L2 frequency channel. This fact is expressed in details in reference [30]. A diagram of open loop tracking method in the satellite receiver is depicted in Fig.2.

In 2005, this method was implemented in the blackjack receiver (this receiver was built based on geodetic receiver Turbo Rogue) for the first time and then it was used in IGOR receiver in COSMIC satellite in 2006. Some applied models for open-loop tracking are Sokolovskiy model, [3] Christensen model [31] and the implemented model in Scientific Application Satellite-C (SAC-C) satellite.

The Doppler model estimation has to be accomplished in the satellite receiver before the acquisition of any occultation event. A controller signal is composed of the Geometric Doppler and Atmospheric Doppler. In the OL mode, the signal frequency is down-converted by an oscillator numerically controlled by a phase model independent from the measured signal, i.e. without the feed-back. Because it is always possible to provide a phase model predicting the Doppler frequency of the signal with an accuracy of 10–15 Hz, the 50 Hz sampling rate is sufficient for the correct retrieval of the signal phase [3]. A down converter converts the received signals into a suitable frequency by applying this controller signal. Subsequently, this signal goes through a low pass filter and is then sampled. In tracking the signal, the rate of Doppler variation is also important in addition to Doppler. As mentioned in the literature, the closed-loop tracking is possible if the Doppler variation rate is less than 3 KHz/s, whereas in rates higher than 3 KHz/s, the utilization of open-loop tracking is necessary.

3- Atmospheric Doppler

It is necessary to compute from the excess phase delay the Atmospheric Doppler, which is not Doppler in the conventional sense, but rather the time derivative of the excess phase delay on the signal caused by the atmosphere. The sign convention for Atmospheric Doppler employed in this work is that increasing range rate or increasing excess phase (as in a descending occultation) gives negative Doppler.

Note that in previous works, such as [3], the total Doppler was measured, then the Geometric Doppler was calculated and subtracted from the total, and the Atmospheric Doppler was

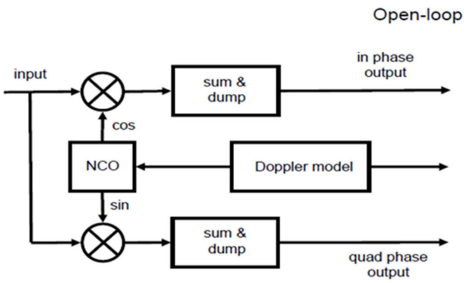

Fig. 2. The structure of an open-loop receiver

obtained. Then, the atmospheric parameters were obtained by utilizing this Atmospheric Doppler. But here, for OL tracking, the process is inversed. We model the Atmospheric Doppler by atmospheric parameters or by data archived in databases. Then, we calculate the Geometric Doppler and add it to atmospheric one to gain the total Doppler, and we put the total in Doppler model block. This is a different approach to related works such as [32,3].

Information regarding the occurred occultation is stored in databases which can be accessed through the following websites:

1) http://cdaac-www.cosmic.ucar.edu/cdaac
CDAAC database contains the raw and processed data of 8 occultation missions in addition to COSMIC mission. CDAAC is the abbreviation of COSMIC Data Analysis & Archive Center.

2) http://genesis.jpl.nasa.gov/genesis
In this database several missions including COSMIC are covered. It can be freely accessed.

In these two databases, excess phase data given in meter is related to the excess Doppler, Δf as follows [2]:

$$\Delta f = -(1/\lambda) d\tilde{L}/dt \quad (1)$$

Where ($\tilde{L}$) is the excess phase, measured accurately as a function of time in the databases and λ is the wavelength. Therefore the excess Doppler (Atmospheric Doppler) is obtained by calculating the variation rate of the excess phase in time, where the wavelength is given as follows:

$$\lambda = \frac{c}{f_{L1}} \quad (2)$$

Where $c=3\times10^8$ m/s is the speed of light and f_{L1}=1.5742 GHz is the GPS L1 carrier frequency.

The phenomenon of Radio latency measurements at the first amplitudes of A1 and A2 and phases of L1 and L2 from each transmitting signals are measured. Then by using Radio Holographic and orbital data of satellites and by supposing spherical symmetry in on way mediums, α_1 and α_2, the bending angles will be calculated.

$$A\exp(i\Phi(x)) \rightarrow \begin{bmatrix} \textit{Back propagation} \\ \textit{Sliding spectrum} \\ \textit{Canonical transform} \\ \textit{Full spectrum inversion} \end{bmatrix} \rightarrow \alpha(a) \quad (3)$$

Using ionospheric corrections, the bending angle without ionospheric error will be obtained. Then, by using the weather condition data in high height and Abel transmission, the refraction characteristics will be defined [3].

$$\alpha(a) \rightarrow \left\{ \begin{array}{l} \alpha(a) = -2a\int_{r_0}^{\infty} \frac{d\ln n}{\sqrt{n^2 r^2 - a^2}} dr \leftrightarrow n(r_0) \\ = \exp\left(\frac{1}{\delta} \int_a^{\infty} \frac{\alpha(x)}{\sqrt{x^2 - a^2}} dx \right) \\ r_0 = \frac{a}{n(r_0)}, \; N(r_0) = 10^6 \times (n(r_0) - 1) \end{array} \right\} \rightarrow N(r) \quad (4)$$

At the end of this process by using weather condition data, that are conventionally the temperature data, the atmospheric data will be obtained.

Refraction coefficient is related directly to the density of the electrons in the ionosphere layer, and it is related to the pressure, temperature, water vapor in pure atmosphere[30]:

$$N = a_1 \frac{P}{T} + a_2 \frac{P_{wv}}{T^2} - b \frac{n_e}{f^2} \quad (5)$$

Where a_1=77.6 ,a_2=3.73*10^5, b=40.3*10^6, T, the temperature, in Kelvin, p_{wv} , pressure in mb and n_e, density of electron in $1/m^3$.

The first two relations are the refraction in the pure part and the third relation is about the electron density in the ionosphere layer.

The amount of TEC (Total Electron Count) is obtained by measuring in two frequencies (F1 and F2) with a LEO satellite receiver, according to this equation [33]:

$$TEC = \frac{1}{40.3} \frac{F_1^2 F_2^2}{F_1^2 - F_2^2} (L_1 - L_2) \quad (6)$$

In this relation, L1 and L2 are the delays of the F1 and F2 signals passing the ionosphere layer.

4- Atmospheric Doppler Feature

In this section, the atmospheric Doppler for occultation occurred between COSMIC satellites and GPS satellites in 2013, occurred in Tehran, as an example is computed and then more observations and more accurate Doppler can be obtained by this method for more COSMIC satellites and also other mission. In this method, we use the measured excess phases in CDAAC database; then, differentiate them based on equation (1) to gain the atmospheric Doppler. In this approach, we don't use the atmospheric models to estimate the Doppler, and we use the archived data of a similar previous occultations to obtain the Atmospheric Doppler for current and coming occultations.

In CDAAC database, we can search the occurred radio occultations at latitude and longitude of defined places like Tehran. Then, we choose the COSMIC1 as the LEO satellite and the year 2013 to limit the results. So CDAAC shows eight occultations. In Table 2, the time, the location, and the GPS number of the each occultation are shown. In Figs.3 and 4 you can see the details of atmospheric Doppler in sitting and rising occultation on 13 March 2013 and 17 August 2013 in Tehran, Iran respectively related to information in rows 2 and 4 and in Fig 5 is depicted the phase acceleration.

Now, we will investigate the Doppler by CDAAC database for different atmospheric conditions and one can see the effect of the climate on the atmospheric Doppler.

Table 1. Different type of open loop tracking [1]

Sampling rate	Total data in one day	Comments
20 MHz	800 GB	No Doppler prediction
2 KHz	300 MB	Geometric Doppler model
50 Hz	50 MB	Geometric and Atmospheric Doppler model

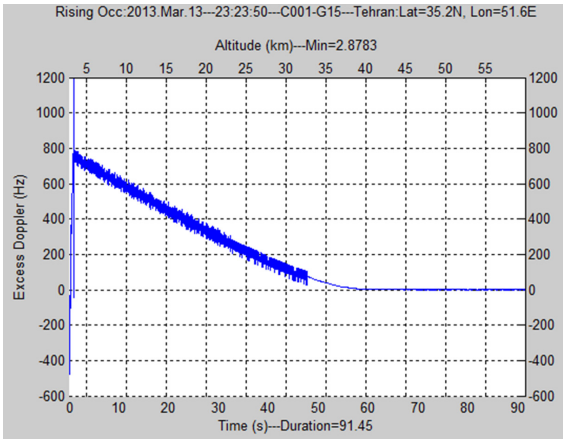

Fig. 3. A rising occultation related to 13 March 2013, at 23:23:50, between COSMIC1 and GPS#15. The location is in Tehran area at 35.2N latitude and 51.6E longitude. The minimum altitude is 2.8783 km and the maximum Doppler shift is 787.0Hz.

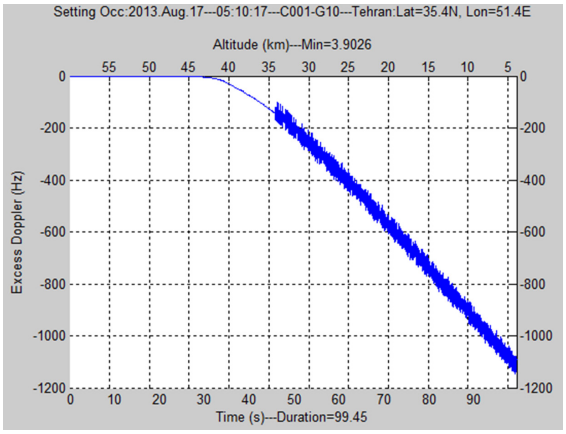

Fig. 4. A setting occultation related to 17 August 2013 at 05:10:17, between COSMIC1 and GPS#10. The location is in Tehran area at 35.4N latitude and 51.4E longitude. The minimum altitude is 3.9026 km and the maximum Doppler shift is 1144.8 (Hz).

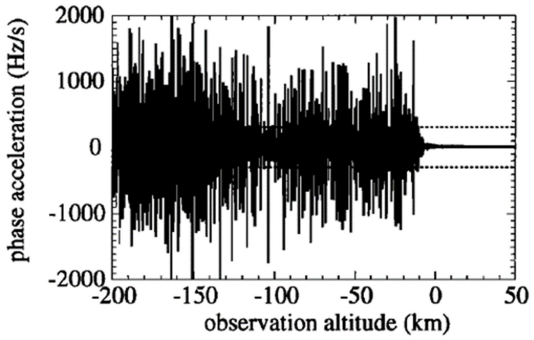

Fig. 5. First derivative (phase acceleration) of Excess Doppler

For more investigation about the features of atmospheric Doppler, we collect the data for occultations events in different locations, time, and different seasons, and analyses the amount of these types of Doppler. The results are shown in Table 3.

The detailed information of each occultation is archived in its exclusive files as: atmPrf.nc and atmPhs.nc. In atmPrf.nc the excess phase, $\tilde{L}$, is expressed in terms of time and in atmPhs.nc, the excess phase is expressed in terms of altitude. The matrices of time, excess phase, and altitude are extracted from the atmPrf.nc and atmPhs.nc files of each occultation. Then the atmospheric Doppler is computed by the equations (1) and (2).

We consider numbers 2 and 4 of the eight considered occultations as following cases, a) rising occultation in the initial stages of acquiring the signal and b) a setting occultation. The excess Doppler with respect to the altitude (the distance between the tangent point and Earth's surface) in the time of occultation event occurrence is depicted in Figs. 3 and 4. In the case of rising occultation in the initial stages of acquiring the signal, some overshoots in Doppler are observed, due to the start of receiving a multipath affected and weak signal.

The excess Doppler profiles plotted in Figs. 3 and 4 exhibit striking 50 Hz fluctuations at altitudes below 32 km and 34 km, respectively. These onset altitudes approximately coincide with the transitions altitudes from closed-loop to open-loop mode tracking (vice versa for the rising occultation). The most likely explanation for the observed fluctuations is a failure to remove the phase jumps which are induced by the 50 Hz data modulation.

In closed-loop mode the demodulation is taken care of by the receiver; carrier phase data acquired in open-loop mode, however, need to be corrected for during post-processing (see,. e.g., Figs. 5 and 6 in Sokolovskiy et al., 2009, reference [9]). In this case the observed fluctuations are not of atmospheric origin. In lower troposphere, the derivative of Doppler has a variation of more than ±2Khz as shown in Fig 5 [34].

5- Geometric Doppler

Geometric Doppler (Doppler expected in the absence of the atmosphere) has an explicit definition and can be obtained by determining the orbital parameters of LEO and GPS.

The relation between the Geometric Doppler frequency and the relative satellite-receiver motion is (neglecting the oscillator effects and ionospheric effect):

$$f_{Geometric\ Doppler} = \frac{v_{r,s}}{c} f_0 \tag{7}$$

With $f_{Geometric\ Doppler}$ being the Geometric Doppler effect, $v_{r,s}$ the relative satellite-receiver velocity, f_0 the carrier wave frequency. The Geometric Doppler, $d_{Geometric\ Doppler}$, is simply the difference of the projection of the two satellite velocities onto the inter-satellite vector:

$$d_{Geometric\ Doppler} = v_{GPS}\cos\phi_{GPS} + v_{LEO}\cos\phi_{LEO} \tag{8}$$

With ϕ_{GPS} being the angle between the velocity vector of the GPS satellite and the inter satellite vector, and ϕ_{LEO} being the corresponding angle for the LEO. All quantities are known or can be computed from the satellite positions and velocities. Note that the actual geometry can vary significantly from that depicted, depending on the direction of the GPS satellite velocity, and whether the occultation is rising (LEO approaching the GPS satellite) or descending (LEO receding from the GPS satellite).

In this paper, a variety of scenarios for a LEO satellite in STK (System Tool Kit) software are defined to show the nature of Geometric Doppler in the event of an occultation. Systems Tool Kit (formerly Satellite Tool Kit), is a physics-based software package from Analytical Graphics, Inc. that allows engineers and scientists to perform complex analyses of ground, sea, air, and space assets, and share results in one integrated solution. As it is shown in Table 5, the GPS satellites include 32 satellites in 6 different planes.

Considering Table 5, the satellites with GPS-RO payload are in altitudes about 500-800 km. So, eight missions in 450 to 800km altitudes are defined in STK and the transmitted signal of GPS satellites is saved for one day by locating the receiver on the LEO satellite.

According to the developed information, the Geometric Doppler and first deviation in three cases with three different places are depicted in the Figs.6-8. The scenarios are three satellites in altitudes of 450, 600, and 800 in three plane A, B, and D, respectively.

The first derivations of Doppler shift values are very important for receiver designing and selecting tracking method. If the values of the first derivations of Doppler shift is more than 300Hz/s, PLL tracking method cannot be used [35]. This means if there were only the geometry Doppler shift, the tracking would be possible just by PLL tracking. But now, since there are two Doppler shifts, if the variations are more than 300Hz/s, the tracking has to be open loop.

For studying the Geometric Doppler, resulting from the relative velocity vectors of the GPS and LEO satellite, the Doppler and its first derivatives are simulated based on the defined mission of the LEO satellite in STK. In this simulation, we should consider the 6 different orbital planes of the GPS satellites according to the Table5. As expected, the acquired signals of the satellites in the same planes meet the same Doppler pattern only with the time shift.

According to Figs.6, 7, and 8, we see that the quantity of Doppler depends on the satellite since the GPS satellites are in 6 planes, so the observed Doppler from 32 satellites has 6 different patterns and therefore just these 6 models shall be investigated.

6- Geometric Doppler Nature

Other considered subjects are the maximum and minimum values of the Doppler shift. As seen, by increasing the altitude, the maximum and minimum values of the Doppler shift decrease. This point is repeated in all planes. The reason is that by increasing the altitude of the LEO satellite, the two satellites' distance decreases and the LEO satellite velocity also decreases. Therefore, the relative velocity of the satellites and the Doppler decrease.

As the altitude of the LEO enhances, the duration of the two satellite observation enhances and it occurs in all GPS orbital planes. The signal cutoff duration is also lower, because when the LEO takes distance from the earth, the duration of being in the shadow of the earth decreases. So the observation period enhances.

Table 2. The ROs between COSMIC1 and GPS satellites in 2013 at Tehran region

#	Occurrence time	Location	GPS#	Type	Min. Altitude	Max. Doppler
1	5th Feb. 2013 04:27:54	35.5 N 51.7 E	G25	rising	3.75 (km)	323 (Hz)
2	13th Mar. 2013 23:23:50	35.2 N 51.6 E	G15	rising	2.88 (km)	787 (Hz)
3	19th Mar. 2013 20:37:06	34.4 N 51.5 E	G09	rising	3.26 (km)	812 (Hz)
4	17th Aug. 2013 20:08:01	35.4 N 51.4 E	G10	setting	3.90 (km)	1145 (Hz)
5	31st Mar. 2013 05:10:17	35.4 N 51.5 E	G07	setting	3.82 (km)	829 (Hz)
6	23rd Sep. 2013 12:36:44	35.6 N 51.9 E	G16	rising	3.51 (km)	844 (Hz)
7	17th Oct. 2013 04:25:39	34.7 N 51.0 E	G10	rising	1.95 (km)	698 (Hz)
8	26th Dec. 2013 09:38:10	34.4 N 51.5 E	G31	rising	3.12 (km)	791 (Hz)

Table 3. Doppler shifts for different climates

#	Occurrence time	Location	Satellites	Type	Min. Altitude	Max. Doppler
			Tehran (Mild)			
1	4th Jan. 2014 14:35	35.9 N 51.7 E	G02-CO04	setting	3.75 (km)	1005 (Hz)
2	17th Mar. 2014 14:36	35.9 N 51.8 E	G10-CO04	setting	4.24 (km)	523 (Hz)
3	22nd Mar. 2014 13:45	35.4 N 51.5 E	G03-CO04	rising	3.84 (km)	1216 (Hz)
4	12th Jan. 2014 07:55	35.4 N 51.4 E	G16-CO05	setting	3.39 (km)	863 (Hz)
			Dasht-e Kavir (Dry)			
1	19th Feb. 2014 01:00	34.5 N 55.0 E	G16-CO01	setting	1.47 (km)	945 (Hz)
2	15th Jan. 2014 07:26	34.6 N 55.4 E	G15-CO02	rising	1.73 (km)	784 (Hz)
3	26th Apr. 2014 20:18	35.0 N 55.9 E	G18-CO02	setting	1.84 (km)	938 (Hz)
4	4th Feb. 2014 16:23	34.7 N 55.1 E	G27-CO05	setting	2.81 (km)	918 (Hz)
5	28th Jan. 2014 01:42	35.1 N 55.4 E	G10-CO06	rising	0.36 (km)	782(Hz)
			Caspian Sea Margins (Moist with cold winter)			
1	12th Apr. 2014 05:09	37.7 N 49.4 E	G19-CO01	setting	2.19 (km)	1166 (Hz)
			Persian Gulf Margins (Tropical Moist Climates)			
1	19th Jan. 2014 19:44	25.7 N 54.2 E	G05-CO01	setting	0.87 (km)	896 (Hz)
2	8th Feb. 2014 23:32	26.7 N 54.6 E	G04-CO06	rising	0.41 (km)	761 (Hz)

Table 4.some GNSS-RO Mission

Altitude (km)	Year of launch and lifespan	Mission
500	11/2000 About 5 years	CHAMP
705	11/2000 About 3 years	SAC-C
500	5/2002 About 5 years	GRACE
805	9/2005 About 5 years	COSMIC FORMOSAT 3
514	7/2005 About 5 years	TerraSAR-X
831	5/2007 About 5 years	METOP
828	3/2011 About 10 years	NPOESS
780	from 2014 to 2017 8 to 10 years	Iridium NEXT

Table 5. GPS satellite in 6 defined plane

Plane	Satellite 1	Satellite 2	Satellite 3	Satellite 4	Satellite 5	Satelllite 6
A	BIIA-12	BIIA-15	BIIA-21	BIIA-28	BIIRM-2	-
B	BIIA-22	BIIA-27	BIIR-05	BIIR-08	BIIRM-3	-
C	BIIA-20	BIIA-24	BIIA-25	BIIR-11	BIIRM-1	-
D	BII-09	BIIA-11	BIIA-23	BIIR-03	BIIR-09	BIIR-13
E	BIIA-10	BIIA-26	BIIR-04	BIIR-07	BIIR-10	-
F	BIIA-14	BIIA-16	BIIA-17	BIIR-02	BIIR-06	BIIR-12

The altitude growth of the receiver satellite does not affect the Doppler and its derivative patterns. The difference of the curves is their broadening, because of the receiver velocity reduction. In fact, by altitude enhancement, repetition duration or period of the patterns increases.

As noted, the purpose of these simulations is to study Geometric Doppler in the event of an occultation. Theoretically, when an occultation occurs, either GPS and LEO satellites see each other or they are out of sight of each other. Therefore, as observed in Fig. 6-8, the points near the signal area are the points of the occultation occurrence area. Accordingly, the number of occultation events in one day depends on the LEO satellite's altitude. Table 6 expresses a statistical analysis of the signal outage situation. This table is obtained by simulation of different missions in one day and counting the disconnections of the Doppler signal, and these numbers show the number of the occurred occultations.

As demonstrated, the amount and pattern of Geometric Doppler is related to the orbital parameters as the height of orbit increases, the maximum of Geometric Doppler decreases. Also, the number of the occultations depends on

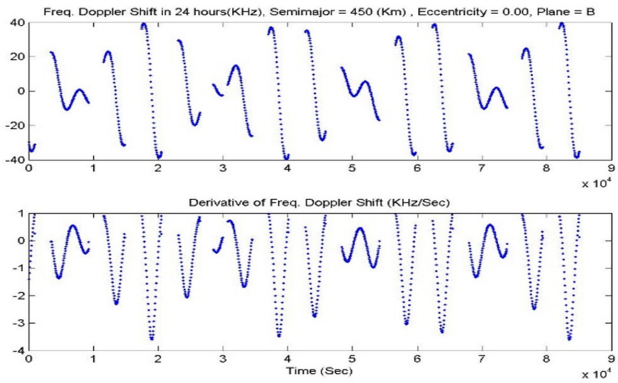

Fig. 6. The Doppler shift and first derivative of Geometric Doppler at LEO satellite in altitude 450 (km)

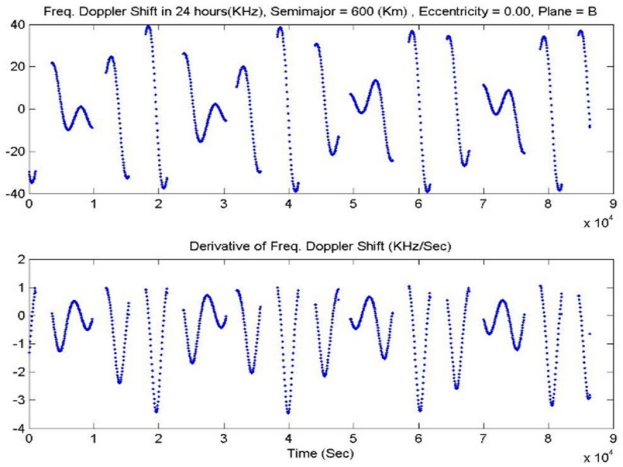

Fig. 7. The Doppler shift and first derivative of Geometric Doppler related to LEO satellite in altitude 600 (km)

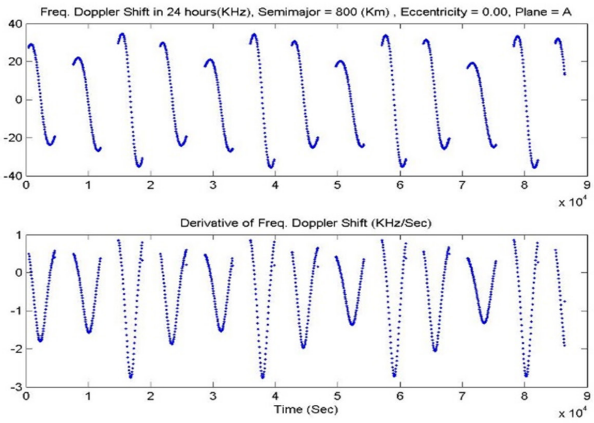

Fig. 8. The Doppler shift and first derivative of Geometric Doppler related to LEO satellite in altitude 800 (km)

the GPS satellite and the orbital altitude. Where the altitude of the LEO orbit is higher, the number of the occurrences is smaller. For example, the computation of the occultation number within one day, with the assumption of receiving from 30 GPS satellites by one LEO satellite, is 720 events for an 800 km altitude orbit and that is 840 for a 450 km altitude. This point affects the required memory and bandwidth of the receiver. But as evident in Fig. 6-8, several events have a very short time, and in practice, they are not received; it is mentioned that about 600 events can be recorded in one day.

Table 6. Number of signal disconnection in different LEO altitude

LEO HEIGHT (km)	1500	800	750	700	650	600	550	500	450
Plane A	20	24	25	25	25	25	25	27	**27**
Plane B	19	25	25	25	26	27	28	29	**29**
Plane C	18	25	25	29	31	32	32	32	**35**
Plane D	18	24	25	26	26	26	26	26	**27**
Plane E	21	25	25	25	25	25	26	26	**26**
Plane F	20	24	25	25	25	26	26	26	**27**
Average per plane	19	24	25	26	26	27	27	28	**28**

In addition, the Doppler value is affected by the orbit altitude. The considerable point is the reduction of the Doppler value by the LEO orbit altitude growth. But it is determined that the on-board receiver of the satellite shall be able to endure for the range of -/+ 50 KHz. The variation of the Doppler in the occultation event area is less than -/+ 1 KHz/sec.

7- Conclusion

In this paper, by using the CDAAC database and STK software, specific information is extracted to achieve the treatment of the Doppler variations and their relation to the time of the event occurrence. According to these evaluations, the Atmospheric Doppler, dependent on the atmospheric conditions and geometrical positions, is so variable. It was also demonstrated that the Geometric Doppler value, which is dependent on the orbital altitude of the LEO, its orbital parameters, and the instant of the occultation occurrence, is a maximum of about +/- 50 KHz. In RO receivers, we need precise Doppler modeling to implement open-loop tracking with minimum rate of sampling and optimum use of satellite bandwidth. By combining the Geometric Doppler and Atmospheric Doppler, the Doppler frequency shift of the RO signal is estimated and can be located in the Doppler model block of an open-loop receiver (Fig.2).

Also by evaluation of first derivation of Doppler we reach to deep understanding of changing of receiver mode to OL or CL related to phase acceleration of received signal.

References

[1] W. H. Bai, Y. Q. Sun, Q. F. Du, G. L. Yang, Z. D. Yang, P. Zhang, Y. M. Bi, X. Y. Wang, C. Cheng and Y. Han, "An introduction to the fy3 gnos instrument and mountain-top tests," Atmos. Meas. Tech., vol. 7, p. 1817–1823, June 2014.

[2] S. Sokolovskiy, "Method and System for determining The phase and amplitude of a radio occultation signal " U.S. Patent 6,731,906 B2, May 2004

[3] S. Sokolovskiy, "Tracking Tropospheric Radio Occultation Signals from Low Earth Orbit," Radio Sci., vol. 36, no. 3, p. 483–498, June 2001.

[4] S. Sokolovskiy, C. Rocken, W. Schreiner, D. Hunt and J. Johnson, "Post processing of l1 gps radio occultation signals recorded in open-loop mode," Radio Sci., vol. 44, p. 1–13, May 2009.

[5] S. Sokolovskiy, C. Rocken, D. Hunt, W. Schreiner, J. Johnson and D. Masters, "GPS Profiling of the Troposphere from Space: Inversion and Demodulation of the open-loop radio occultation signals," Geophysical Research Letters, vol. 33, no. 3, p. 483–498, April 2006.

[6] C. O. Ao, G. A. Hajj, T. K. Meehan, D. Dong, B. A. Iijima, A. J. Mannucci and E. R. Kursinski, "Rising and Setting GPS occultations by use of open-loop tracking," Journal of Geophysical Research: Atmospheres, vol. 114, no. D4, February 2009.

[7] W. Schreiner, C. Rocken, S. Sokolovskiy, S. Syndergaard and D. Hunt, "Estimates of the Precision of GPS Radio Occultations from COSMIC/FORMOSAT-3," Geophysical Research Letters., vol. 34, 2007.

[8] R. A. Anthes and e. al., "The COSMIC/FORMOSAT-3 mission: Early results," Bull. Am. Meteorol. Soc., vol. 89, p. 313–333, 2008.

[9] S. B. Healy and J. N. The´paut, "Forecast Impact Experiment with GPS Radio Occultation Measurements," Q.J.R. Meteorol. Soc., vol. 132, p. 605–623, 2006.

[10] L. Cucurull, J. C. Derber, R. Treadon and R. J. Purser, "Preliminary Impact Studies using Global Positioning System radio occultation profiles at NCEP," Mon. Weather Rev., vol. 136, p. 1865– 1877, 2008.

[11] L. B. Hande, S. T. Siems, M. J. Manton and D. H. Lenschow, "An evaluation of COSMIC Radio Occultation Data in the Lower Atmosphere over the Southern Ocean," Atmos. Meas. Tech., vol. 8, no. 1, pp. 97-107, Jan 2015.

[12] M. E. Gorbunov, "Radio-Holographic Analysis of Microlab-1 Radio Occultation Data in the Lower Troposphere," Journal of Geophysical Research., vol. 107, no. D12, 2002

[13] E. R. Kursinski, G. A. Hajj, S. S. Leroy and B. Herman, "The GPS Radio Occultation Technique," Terr. Atmos. Oceanic Sci., vol. 11, no. 1, p. 53–114, 2000.

[14] M. E. Gorbunov, "Canonical Transform Method for Processing Radio Occultation Data in the Lower Troposphere," Radio Sci., vol. 37, no. 5, 2002.

[15] M. E. Gorbunov and L. Kornblueh, "Analysis and validation of GPS/MET Radio Occultation Data," Journal of Geophysical Research, vol. 106, no. D15, p. 161–169, 2001.

[16] A. S. Nielsen, A. S. Jensen, M. S. Lohmann, H. H. BenFull, "Spectrum Inversion of Radio Occultation Signals," Radio Sci., vol. 38, no. 3, 2003.

[17] M. E. Gorbunov and L. Kornblueh, "Analysis of Wave Fields by Fourier Integral Operators and their Application for Radio Occultations," Journal of Geophysical Research, vol. 39, 2004.

[18] A. S. Jensen, M. S. Lohmann, H. H. Benzon and A. S. Nielsen, "Geometrical Optics Phase Matching of Radio Occultation Signals," Radio Sci., vol. 39, 2004.

[19] C. O. Ao, T. K. Meehan, G. A. Hajj, A. J. Mannucci and G. Beyerle, "Lower Troposphere Refractivity bias in GPS Occultation Retrievals," Journal of Geophysical Research., vol. 108, no. D18, 2003.

[20] G. Beyerle, M. E. Gorbunov and C. O. Ao, "Simulation studies of GPS radio occultation measurements," Radio Sci., vol. 38, no. 5, 2003.

[21] K. Hocke, A. G. Pavelyev, O. I. Yakovlev, L. Barthes

and N. Jakowski, "Radio Occultation Data Analysis by the Radio Holographic method," J. Atmos. Sol-Terr. Phys, vol. 61, p. 1169–1177, 1999.

[22] S. Sokolovskiy, C. Rocken, W. Schreiner and D. Hunt, "On the uncertainty of Radio Occultation Inversions in the lower troposphere," Journal of Geophysical Research, 2010.

[23] C. Rocken and e. al., "Analysis and validation of GPS/MET data in the Neutral Atmosphere," Journal of Geophysical Research., vol. 102, no. D25, pp. 29,849–29,866, 1997.

[24] C. Marquardt, K. Schollhammer, G. Beyerle, T. Schmidt, J. Wickert and C. Reigber, "Validation and Data Quality of CHAMP Radio Occultation Data, in First CHAMP Mission Results for Gravity," Magnetic and Atmospheric Studies, p. 384–396, 2003.

[25] G. A. Hajj, C. O. Ao, B. A. Iijima, D. Kuang, E. R. Kursinski, A. J. Mannucci, T. K. Meehan, L. J. Romans, M. de la Torre Juarez and T. P. Yunck, "CHAMP and SAC-C Atmospheric Occultation Results and Inter Comparisons," Journal of Geophysical Research., vol. 109, no. D06109, 2004.

[26] S. V. Sokolovskiy, "Effect of super refraction on inversions of Radio Occultation Signals in the Lower Troposphere," Radio Sci., vol. 38, no. 3, 2003.

[27] F. Xie, S. Syndergaard, E. R. Kursinski and B. Herman, "An Approach for Retrieving Marine Boundary Layer Refractivity from GPS occultation data in the Presence of Super-Refraction," J. Atmos. Oceanic Technol., vol. 23, p. 1629–1644, 2006.

[28] C. O. Ao, "Effect of Ducting on Radio Occultation measurements: An Assessment based on High-Resolution Radio sonde soundings," Radio Sci., vol. 42, no. RS2008, 2007.

[29] G. Beyerle, S. Heise, T. Schmidt, J. Wickert and M. Rothacher, "Tracking GPS radio Occultation Signals in the Lower Troposphere: CHAMP Observations and Simulation Studies," DMI Technical Report 05-11, 2005.

[30] S. Gleason and D. Gebre-Egziabher, GNSS Applications and Methods, Boston: Artech House , 2009.

[31] M. Bonnedal, A. Carlström, J. Christensen and M. Sust, "Apparatus and Method for Performing Open Loop Tracking of a Signal". USA Patent US6720916 B2, 13 April 2004.

[32] E. R. Kursinski, "Observing Earth's Atmosphere with Radio Occultation Measurements using the Global Positioning System," Journal of Geophysical Research: Atmospheres, vol. 102, no. D19, pp. 23429-23465, 1997.

[33] Man Feng, Detection of high latitude ionospheric Irregularities from GPS, Ph.D. Dissertation, Radio Occultation Department of Geometrics Engineering , University of Calgary, May 2010.

[34] Sokolovskiy, Sergey, "Modeling and Inverting Radio Occultation Signals in the Moist Troposphere", Radio Sci., vol. 36, no. 3, pp. 441-458, 2001.

[35] Sergey, Sokolovskiy,"Modelling of tropospheric RO signals, Acquisition of the Tropospheric RO Signals" UCAR –COSMIC project.

Please cite this article using:

L. Mohammadi, S. Amiri, G.R. MohammadKhani,"Evaluation of Geometric and Atmospheric Doppler for GNSS-RO Payloads", *AUT J. Elec. Eng.*, 49(1)(2017)85-94.

DOI: 10.22060/eej.2016.12054.5030